CHEMICAL ENGINEERING TRANSACTIONS
VOL. 106, 2023
A publication of AIDIC
The Italian Association of Chemical Engineering
Online at www.cetjournal.it
Guest Editors: Jeng Shiun Lim, Nor Alafiza Yunus, Peck Loo Kiew, Hon Huin Chin

ISBN 979-12-81206-05-2; **ISSN** 2283-9216
DOI: 10.3303/CET23106165

Oil Adsorption using Activated Carbon Derived from Rubber Seed Kernels (*Hevea brasiliensis*)

Muhammad Aisar Harraz Aswadi[a], Hairul Nazirah Abdul Halim[a,b,*], Nur Farhana Najwa Nasaruddin[a], Siti Khalijah Mahmad Rozi[a,b], Zulfakar Mokhtar[a], Lian See Tan[c], Nurfatehah Wahyuny Che Jusoh[c]

[a]Faculty of Chemical Engineering & Technology, Universiti Malaysia Perlis (UniMAP), Kompleks Pusat Pengajian Jejawi 3, 02600 Arau, Perlis, Malaysia
[b]Center of Excellence for Biomass Utilization, Universiti Malaysia Perlis (UniMAP), Kompleks Pusat Pengajian Jejawi 3, 02600 Arau, Perlis, Malaysia
[c]Department of Chemical and Environmental Engineering (CHEE), Malaysia - Japan International Institute of Technology (MJIIT), Universiti Teknologi Malaysia (UTM), Jalan Sultan Yahya Petra (Jalan Semarak), 54100 Kuala Lumpur, Malaysia
hairulnazirah@unimap.edu.my

Oil pollution from food industries is one of the major environmental concerns nowadays. Improper management and disposal of cooking oils into the drainage system can have undesirable effects on the environment. However, one of the best ways to treat oil pollution is adsorption using activated carbon. In this study, rubber seed kernels (RSKs) were used to produce activated carbon via impregnation with 10 and 15 wt.% phosphoric acid (H_3PO_4). Then, the chemically impregnated RSKs were carbonised at 300, 400, and 500 °C for 1.5 h. The performance of the synthesised rubber seed kernel activated carbon (RSKAC) was evaluated based on its oil adsorption capacity. Samples of raw RSKs and RSKAC were analysed using Scanning Electron Microscopy (SEM) and Fourier-transform Infrared (FTIR) spectroscopy. The results showed that RSK sample impregnated with 10 wt.% H_3PO_4 and carbonised at 500 °C has the highest oil adsorption capacity of 0.896 ± 0.042 g/g. The SEM results showed that the RSKAC sample has more pores than the RSK sample. FTIR spectra of RSKAC revealed that peaks associated with four functional groups (O-H, C-H, C-O, and C=O) were reduced, or disappeared after undergoing H_3PO_4 activation. These findings revealed that RSKAC has the potential to be utilised as an adsorbent for oil adsorption.

1. Introduction

Used cooking oil either from restaurants, or homes is commonly discarded into drains without any prior treatment. Vegetable oils and animal fats, along with their components, may have negative physical effects on the environment, such as suffocating plants and animal due to oxygen deprivation, forming toxic products, contaminating existing and future food supplies, producing rancid odours, and clogging water treatment plants. Hence, a competent oil removal system is important for treating wastewater to avoid harmful effects on the environment.

Adsorption is one of the favourable methods for treating oil in wastewater. Adsorption is the process through which an ion, or a molecule in a liquid, or gaseous phase retains on a solid surface (Rathi & Kumar, 2021). According to Fu et al. (2015), adsorption is favoured over other methods because of its ease of use and simplicity, low-cost operation, flexible, simple designs, and insensitivity to contamination. Adsorbents commonly used in this process include activated carbon, silica gel, and zeolite. Activated carbon can be synthesised from materials with a high carbon content, as it should be porous, adsorptive, strong, with physicochemical stability, and reactive. It also has a large surface area that is distinguishable from elemental carbon based on the oxidised carbon atoms at the inner and outer surfaces (Yahya et al., 2015). However, Azam et al. (2020) reported that conventional activated carbons are expensive due to high production costs. Taking this into consideration, the

Paper Received: 09 March 2023; Revised: 15 July 2023; Accepted: 30 September 2023
Please cite this article as: Aswadi M.A.H., Halim H.N.A., Nasaruddin N.F.N., Rozi S.K.M., Mokhtar Z., Tan L.S., Jusoh N.W.C., 2023, Oil Adsorption using Activated Carbon Derived from Rubber Seed Kernels (Hevea brasiliensis), Chemical Engineering Transactions, 106, 985-990 DOI:10.3303/CET23106165

search for cheaper materials and easy availability has turned researcher's direction towards utilising biomass as activated carbon.

Thus, rubber seed kernels (RSKs) can be used to produce activated carbon, as they can be found in abundance in Malaysia. RSKs consist of 64.5% carbon material, which make them potential candidates as activated carbon (Hassan et al., 2014). According to the report by the Malaysian Rubber Board (2021), Malaysia has a total of 1,098,460 hectares of natural rubber that produced 514,702 t of natural rubber in 2020. This means that a huge amount of rubber seeds has been produced, but only some were planted, while the rest was thrown away. Recently, numerous research studies exploiting waste products have been conducted to develop agro-based activated carbon for oil adsorption, such as sawdust (Rajak et al., 2017), peat (AlAmeri et al., 2019), and *Moringa oleifera* Lam (Bispo et al., 2021). Nevertheless, oil adsorption that employs low cost and environmentally friendly activation protocols using RSKs still needs to be addressed. Transforming these rubber seeds into a valuable product, namely, activated carbon, will contribute to zero waste generation and enhance the utilisation of biomass in the country. Therefore, this study used rubber seeds to synthesise activated carbon labelled as rubber seed kernel activated carbon (RSKAC), which was evaluated based on its oil adsorption performance.

2. Methodology

2.1 Materials and chemicals

Rubber seeds were supplied by FAE Supply Sdn. Bhd. and used as the raw material for synthesising activated carbon. Cooking oil (Knife, Malaysia) was used as the adsorbate in this study, while 85% ortho-phosphoric acid (H_3PO_4) and hexane (C_6H_{14}) were purchased from Bendosen and HmbG Chemical (Germany).

2.2 Preparation of raw material

The rubber seeds were cleaned with distilled water to eliminate contamination and debris. Then, the seeds were separated into shells and kernels. The rubber seed kernels (RSKs) were dried at 100 °C for 24 h in an oven, and later soaked for 15 min in hexane to remove any oils. After 15 min, the oils and hexane were removed, and the RSKs underwent drying for another 2 h. Then, the seeds were ground and sieved to 1,000 µm in size, and safely stored for the next step.

2.3 Chemical activation and carbonisation

Approximately 20 g of RSKs was soaked in 100 mL of different H_3PO_4 concentrations (10 and 15 wt.%) for 24 h to undergo chemical activation. Then, the soaked RSKs were dried in the oven at 100 °C for 1 h. The RSKs were further carbonised at 300, 400, and 500 °C for 1.5 h to produce activated carbon. The last step was to wash the rubber seed kernel activated carbon (RSKAC) with distilled water to eliminate remaining chemicals until pH readings stabilised at pH 6 to 8.

2.4 Effect of RSKAC carbonisation temperature on oil adsorption capacity

One gram of RSKAC was weighed and poured into a nylon teabag. Then, the teabag was submerged in 20 g of cooking oil in a 100 mL beaker. The teabag was taken out of the beaker after a specified time and oil from the teabag was allowed to drip into a filter funnel for 15 min. The initial and final weights of the teabag were recorded to calculate the amount of oil adsorbed into the RSKAC. The oil adsorption capacity, q, was obtained using Eq(1):

$$q = \frac{M_F(g) - M_I(g)}{M_I\,(g)} \quad (1)$$

where M_I and M_F represent the mass of the adsorbents before and after adsorption (g). This experiment was conducted in triplicate, and the average value and standard deviation of q were calculated.

2.5 Characterisation of raw RSKs and RSKAC

Raw RSKs and the RSKAC samples with the highest oil adsorption capacity, as described in Subsection 2.4, were analysed in terms of surface morphology and functional groups. The surface morphology of the samples was analysed using a Hitachi TM3000 Tabletop Scanning Electron Microscope. The chemical structural characteristics were evaluated using a PerkinElmer Spectrum 65 Fourier-transform Infrared Spectrometer. Sample spectra were recorded at 20 scans per sample in the transmittance mode, with 4.0 cm^{-1} resolution ranged between 4,000 and 400 cm^{-1}.

3. Results and discussion

3.1 Effect of carbonisation temperature on oil adsorption capacity

Figure 1 depicts the performance of raw RSKs and the RSKAC produced via chemical activation using 10 and 15 wt% of H_3PO_4 at different carbonisation temperatures (300, 400, and 500 °C).

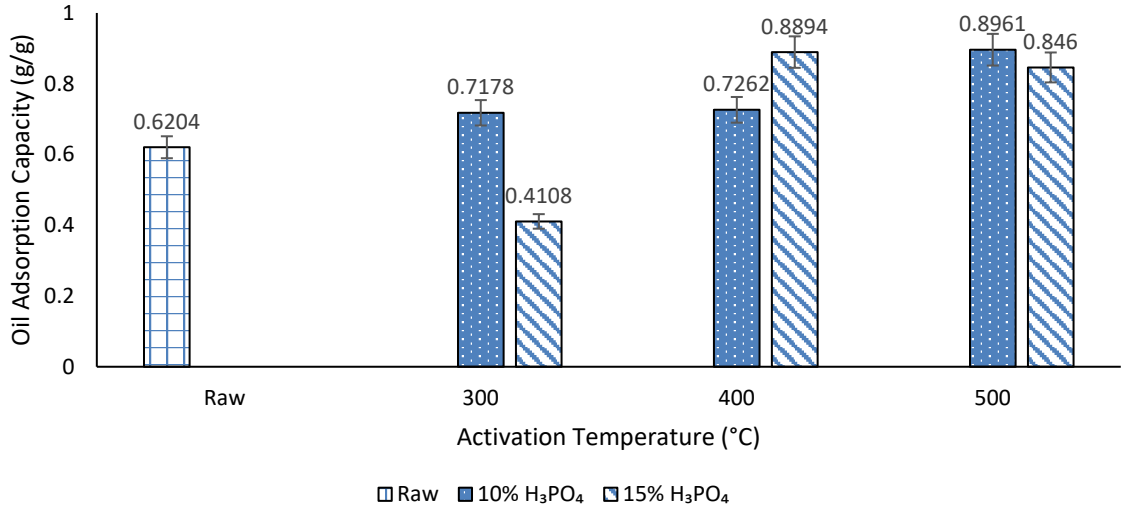

Figure 1: Performance of raw RSKs and the synthesised RSKAC at different activation temperature and H_3PO_4 concentration

The raw RSKs sample recorded an adsorption capacity of 0.6204 g/g. In comparison, higher adsorption capacities were achieved by all RSKAC samples activated by 10 and 15 wt.% of H_3PO_4, except for the sample activated by 15% wt.% of H_3PO_4 at 300 °C. The hydrated 15% wt.% of H_3PO_4 during activation at 300 °C might remained as the salt of H_3PO_4 inside the porous structure of activated carbon, thus occupying a sufficiently large volume. The higher adsorption capacities by RSKAC results were achieved because phosphoric acid, as a dehydrating agent, can penetrate the carbon structure of the RSKs and create small-sized pores during the process. The increased pore volume can be attributed to H_3PO_4, which led to the excellent adsorption capabilities of the RSKAC. This observation was in the agreement with Mbarki et al. (2022), who reported that H_3PO_4 has resulted in the highest adsorption capacity for activated carbon from corn fibres compared to KOH and $ZnCl_2$. They further reported that as an activating agent, H_3PO_4 can hydrolyse, dehydrate, and attack the biomass skeleton, thus, create more pores.

The trend for RSKAC samples activated by 10 wt.% of H_3PO_4 showed that the increasing carbonisation temperature from 300 to 500 °C produced higher oil adsorption capacities. The adsorbed oil was increased from 0.7178 ± 0.0546 to the highest oil adsorption capacity of 0.8961 ± 0.0416 g/g within this range of carbonisation temperature. The elevated carbonisation temperatures have resulted in high pore volumes on the resultant activated carbon. Similar results were reported by Üner and Bayrak (2018), who studied the effect of carbonisation temperature. They found that carbonisation temperature of 500 °C can produce a high volume of mesopores on activated carbon compared to at 400 °C. A high volume of mesopores would increase the active sites available for adsorption and thus, increases the capacity of the activated carbon. In contrast, in the case of RSKAC sample that was activated by 15 wt.% of H_3PO_4, there was a reduction in oil adsorption capacity when the carbonisation temperature was increased from 400 to 500°C, from 0.8894 ± 0.0962 to 0.8460 ± 0.0464 g/g. Beyond 400 °C for 15 wt.%, a secondary shrinkage of the structure might take place as a result of the thermal breakdown of phosphate bonds, which lowers the crosslinking density and helps polyaromatic clusters grow and align. The structure was made more tightly packed and less porous, which then resulted in a slightly lower capacity for oil adsorption (Lim et al., 2020). At 500 °C of carbonisation temperature, chemical activation using 10 wt.% of H_3PO_4 was observed to produce higher oil adsorption capacities compared to using 15 wt.%. This difference could be due to the higher H_3PO_4 concentration damaging the structure of the activated carbon. It could also be due to an incomplete elimination of H_3PO_4 that continued to form phosphate and polyphosphate groups in the pores, hence, blocking oil from entering the pores (Oginni et al., 2019).

3.2 Characterisation of adsorbent

3.2.1 Surface morphology analysis

The morphology of raw RSKs and RSKAC samples was examined using SEM. Figures 2(a) and 2(b) show SEM images of the surfaces of raw RSKs and RSKAC samples with raw RSKs showing a more integrated and smoother surface. As shown in Figure 2(a), the raw RSKs sample shows less pores with fewer cracks, and voids on the rough surface. Meanwhile, chemical activation with 10 wt.% of H_3PO_4 leads to the formation of a network of pores of varying sizes and shapes, as shown in Figure 2(b). This result was obtained from the volatile matter being released during chemical activation, and the carbon elements within the kernels reacted with the activating agent to form micropores and mesopores. This reaction was able to increase the surface area of the RSKAC, which increased its adsorption capacity (Hidayu et al., 2019). The RSKAC sample barely shows a systematised pore development, as seen from the pores in these SEM images. These pores on RSKAC were caused by the evaporated H_3PO_4 during the impregnation process, which left empty spaces (Dizbay-onat et al., 2017). According to Lee et al. (2019), H_3PO_4 can infiltrate deeper into the carbon structure of a material, thus, creating tiny pores.

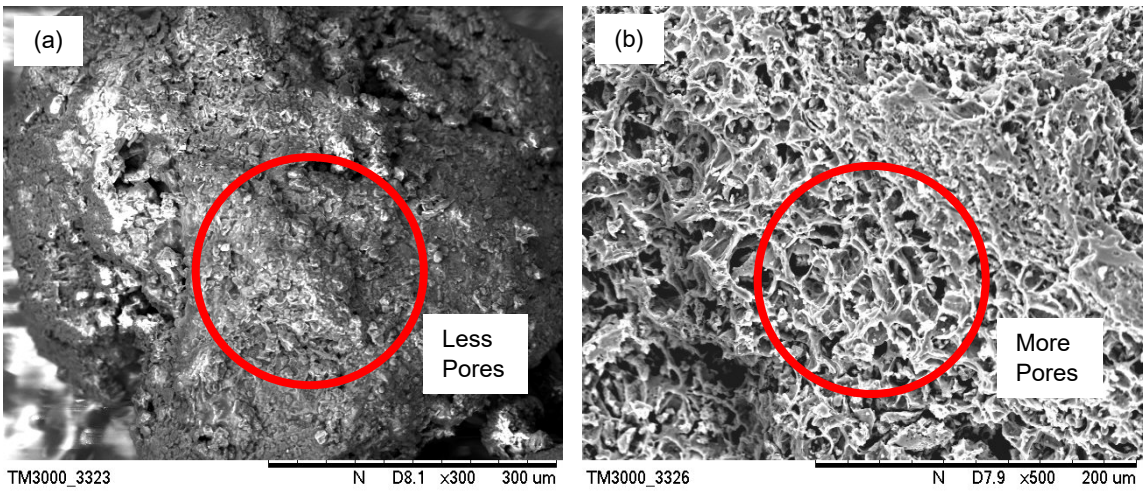

Figure 2: SEM images (a) raw RSKs and (b) RSKAC samples

3.2.2 Functional group analysis

The functional groups of the raw RSKs and RSKAC samples were analysed using FTIR. The FTIR spectra of the assessed samples are shown in Figure 3. The carbonised RSKAC sample had less peaks than the raw RSK sample according to the FTIR spectra. Line A in Figure 3 depicts the strong, broad band, which can be associated to the O-H stretching vibration of carboxyl at 3,316.21 cm^{-1} in the raw RSKs sample (Mokti et al., 2021). Furthermore, the two peaks at 2,924.75 and 2,855.05 cm^{-1} corresponded to asymmetric and symmetric C-H stretching. Meanwhile, the peaks at 1,742.62 and 1,154.92 cm^{-1} can be assigned to C=O and C–O stretching (Maulina and Mentari, 2019). The spectrum of the RSKAC sample is shown in Line B in Figure 3. The peaks associated with the O-H, C-H, C-O, and CO functional groups in this RSKs sample were reduced, or have disappeared following H_3PO_4 activation, which was due to the decomposed organic matters. Furthermore, the intensity of O-H stretching in this sample was decreased compared to the intensity in the raw RSKs sample due to the heating process during carbonisation and activation (Saad et al., 2019). The peaks at 2,924.75 and 2,855.05 cm^{-1} have also reduced to a medium size, which indicated the hydrophobic characteristics of RSKAC after the carbonisation process (Ang et al., 2021). Residue of phosphate compounds remained on the activated carbon's surface; therefore, P-O vibration can be seen at 1,210 cm^{-1} (Kan et al., 2017). These peaks proved the successful formation of RSKAC after RSKs underwent carbonisation and H_3PO_4 activation.

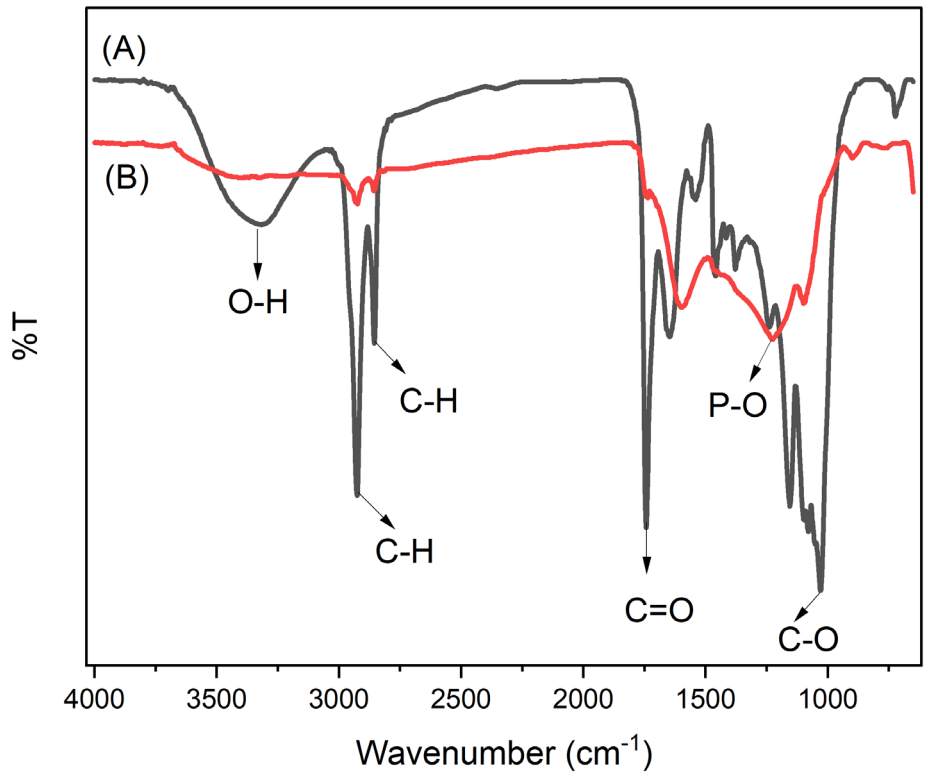

Figure 3: FTIR spectra of raw RSKs (A) and RSKAC(B) samples

4. Conclusions

Activated carbon was derived from rubber seed kernels that were impregnated with 10 and 15 wt.% of H_3PO_4 under different carbonisation temperatures (300, 400, and 500 °C). The performance of the activated carbon was analysed in terms of its oil adsorption capacities. The optimal conditions for producing RSKAC with a high oil adsorption capacity have been demonstrated to be 10 wt.% of H_3PO_4 and carbonised at 500 °C. Next, the structural and morphological analysis results showed more pores on the surface of the synthesised activated carbon compared to on the raw RSKs sample. FTIR results revealed that peaks associated with four functional groups in the RSKAC sample were reduced, or have disappeared following H_3PO_4 activation. This study has shown the potential of converting RSKs into a valuable adsorbent for oil adsorption.

Acknowledgments

The authors are grateful for the National Collaborative Research Grant (CRG) (4B514 and 9023-00014) from Universiti Malaysia Perlis (UniMAP) and Universiti Teknologi Malaysia (UTM) that supported the research activities.

References

AlAmeri K., Giwa A., Yousef L., Alraeesi A., Taher H., 2019, Sorption and removal of crude oil spills from seawater using peat-derived biochar: An optimization study, Journal of Environment Management, 250, 09465.

Ang S.Y., Nasaruddin N.F.N., Halim H.N.A., Rozi S.K.M., Mokhtar Z., Tan L.S., Che Jusoh N.W., 2021, Potential of fatty acid-modified spent tea leaves as adsorbent for oil adsorption, Progress in Energy and Environment, 17, 32–41.

Azam K., Raza R., Shezad N., Shabir M., Yang W., Ahmad N., Shafiq I., Akhter P., Razzaq A., Hussain M., 2020, Development of recoverable magnetic mesoporous carbon adsorbent for removal of methyl blue and methyl orange from wastewater, Journal of Environmental Chemical Engineering, 8(5), 104220.

Bispo M.d.S., Santos J.P.L.d., Santos L.C.L.d., Freitas L.d.S., Bispo D.F., Silva G.F.d., 2021, Synthesis and characterization of activated carbon of *Moringa oleifera* Lam pod and evaluation of its performance in the removal of oils and greases, Journal of Environmental Chemical Engineering, 9, 105965.

Dizbay-onat M., Vaidya U.K., Lungu C.T., 2017, Preparation of industrial sisal fiber waste derived activated carbon by chemical activation and effects of carbonization parameters on surface characteristics, Industrial Crops & Products, 95, 583–590.

Fu J., Chen Z., Wang M., Liu S., Zhang J., Zhang J., Han R., Xu Q., 2015, Adsorption of methylene blue by a high-efficiency adsorbent (polydopamine microspheres): Kinetics, isotherm, thermodynamics and mechanism analysis, Chemical Engineering Journal, 259, 53–61.

Hassan S.N.A.M., Ishak M.A.M., Ismail K., Ali S.N., Yusop M.F., 2014, Comparison study of rubber seed shell and kernel (*Hevea brasiliensis*) as raw material for bio-oil production, Energy Procedia, 52, 610–617.

Hidayu A.R., Sukor M.Z., Mohammad N.F., Elham O.S.J., Azri N.I., Azhar M.A.I., Jalil M.J., 2019, Preparation of activated carbon from palm kernel shell by chemical activation and its application for β-carotene adsorption in crude palm oil, Journal of Physics: Conference Series, 1349, 012103.

Kan Y., Yue Q., Li D., Wu Y., Gao B., 2017, Preparation and characterization of activated carbons from waste tea by H_3PO_4 activation in different atmospheres for oxytetracycline removal, Journal of the Taiwan Institute of Chemical Engineers, 71, 494–500.

Lee C.L., H'ng P.S., Chin K.L., Paridah M.T., Rashid U., Go W.Z., 2019, Characterization of bioadsorbent produced using incorporated treatment of chemical and carbonization procedures, Royal Society Open Science, 6, 190667.

Lee C.L., Chin K.L., H'ng P.S., Rashid U., Maminski M., Khoo P.S., 2021, Effect of pretreatment conditions on the chemical–structural characteristics of coconut and palm kernel shell: A potentially valuable precursor for eco-efficient activated carbon production, Environmental Technology and Innovation, 21, 101309.

Lim A., Chew J.J., Ngu L.H., Ismadji S., Khaerudini D.S., Sunarso J., 2020, Synthesis, characterization, adsorption isotherm, and kinetic study of oil palm trunk-derived activated carbon for tannin removal from aqueous solution, ACS Omega, 5(44), 28673-28683.

Malaysian Rubber Board, 2021, Natural Rubber Statistics (Jan - Mac 2021), Malaysian Rubber Board, <lgm.gov.my/webv2/pdfViewer/nrStatistic> accessed 8.9.2022.

Maulina S., Mentari, V.A., 2019, Comparison of functional group and morphological surface of activated carbon from oil palm fronds using phosphoric acid (H_3PO_4) and nitric acid (HNO_3) as an Activator, IOP Conference Series: Materials Science and Engineering, 505, 012023.

Mbarki F., Selmi T., Kesraoui A., Seffen M., 2022, Low-cost activated carbon preparation from corn stigmata fibers chemically activated using H_3PO_4, $ZnCl_2$ and KOH: Study of methylene blue adsorption, stochastic isotherm and fractal kinetic, Industrial Crops and Products, 178, 114546.

Mokti N., Borhan A., Zaine S.N.A., Zaid H.F.M., 2021, Development of rubber seed shell-activated carbon using impregnated pyridinium-based ionic liquid for enhanced CO_2 adsorption, Processes, 9, 1161.

Oginni O., Singh K., Oporto G., Dawson-Andoh B., McDonald L., Sabolsky E., 2019, Effect of one-step and two-step H_3PO_4 activation on activated carbon characteristics, Bioresource Technology Reports, 8, 100307.

Rajak V.K., Kumar S., Thombre N. V., Mandal A., 2018, Synthesis of activated carbon from saw-dust and characterization for adsorptive separation of oil from oil-in-water emulsion, Chemical Engineering Communications, 205(7), 897–913.

Rathi B.S., Kumar P.S., 2021, Application of adsorption process for effective removal of emerging contaminants from water and wastewater, Environmental Pollution, 280, 116995.

Saad M.J., Chia C.H., Zakaria S., Sajab M.S., Misran S., Rahman M.H.A., Chin S.X., 2019, Physical and chemical properties of the rice straw activated carbon produced from carbonization and KOH activation processes, Sains Malaysiana, 48(2), 385–391.

Üner O., Bayrak Y., 2018, The effect of carbonization temperature, carbonization time and impregnation ratio on the properties of activated carbon produced from *Arundo donax*, Microporous and Mesoporous Materials, 268, 225–234.

Yahya M.A., Al-Qodah Z., Ngah C.W.Z., 2015, Agricultural bio-waste materials as potential sustainable precursors used for activated carbon production: A review, Renewable and Sustainable Energy Reviews, 46, 218–235.